

Enhancing radioisotope identification in gamma spectra with transfer learning

Peter Lalor^{a,*}

^a*Pacific Northwest National Laboratory, Richland, WA 99352 USA*

Abstract

Machine learning methods in gamma spectroscopy have the potential to provide accurate, real-time classification of unknown radioactive samples. However, obtaining sufficient experimental training data is often prohibitively expensive and time-consuming, and models trained solely on synthetic data can struggle to generalize to the unpredictable range of real-world operating scenarios. In this work, we pretrain a model using physically derived synthetic data and subsequently leverage transfer learning techniques to fine-tune the model for a specific target domain. This paradigm enables us to embed physical principles during the pretraining step, thus requiring less data from the target domain compared to classical machine learning methods. Results of this analysis indicate that fine-tuned models significantly outperform those trained exclusively on synthetic data or solely on target-domain data, particularly in the intermediate data regime ($\approx 10^4$ training samples). This conclusion is consistent across four different machine learning architectures (MLP, CNN, Transformer, and LSTM) considered in this study. This research serves as proof of concept for applying transfer learning techniques to application scenarios where access to experimental data is limited.

Keywords: Transfer Learning, Machine Learning, Gamma Spectroscopy, Radioisotope Identification

1. Introduction

The gamma emission spectrum of a specific set of radioisotopes can serve as a fingerprint to perform material identification. The ability to quickly identify the presence, type, and quantity of certain radioisotopes has a wide range of applications in national security, including nuclear forensics, arms control, treaty verification, and counter smuggling. Machine learning is an excellent candidate for gamma spectral analysis due to its ability to efficiently decompose complex spectra. However, obtaining sufficient experimental data to train a machine learning model remains a widespread challenge, as hand labeling a large quantity of experimental spectra is tedious and time-consuming. For this reason, synthetic data is integral to many current machine learning implementations in the field of gamma spectroscopy.

We illustrate the concept of a data hierarchy in Fig. 1, whereby lower levels of data are cheaper and more abundant, but also less representative of a typical operational scenario compared to higher levels. Most prior

*Corresponding author
Email address: peter.lalor@pnl.gov
Telephone: (925) 453-1876

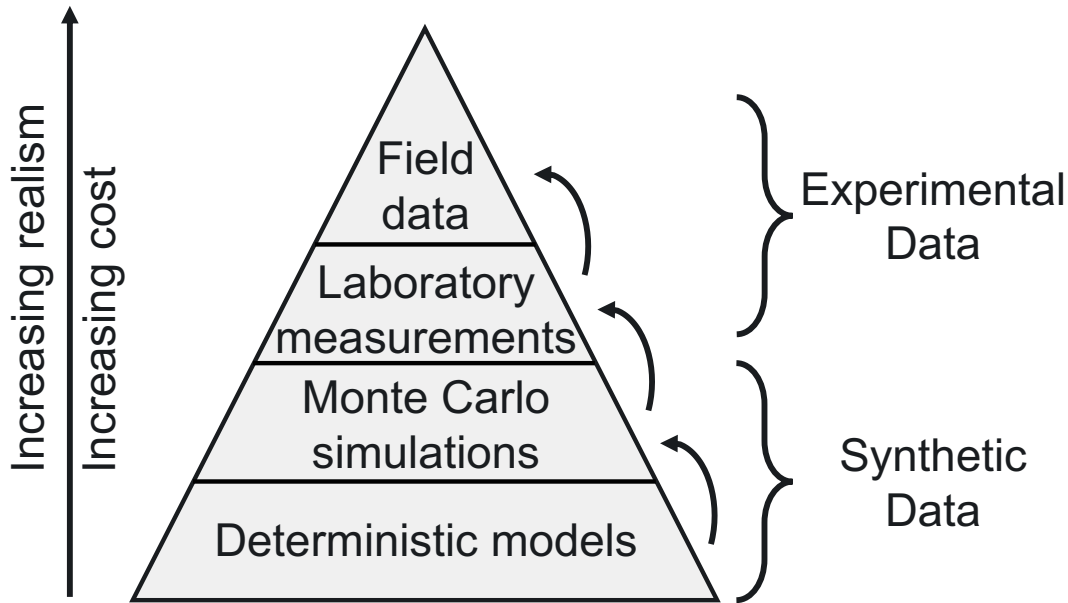


Figure 1: Depiction of a data hierarchy in the field of gamma spectroscopy. Lower levels on the data hierarchy indicate synthetic data, which is cheap and widely available. Higher levels indicate experimental data, which is much more costly but also more realistic for an experimental application. While most existing literature trains machine learning models using data entirely from a single level, we propose leveraging transfer learning techniques (indicated using arrows) to incorporate data across multiple levels.

machine learning studies in the field train a spectral classifier using data entirely from a single level (i.e., training a model using exclusively synthetic data or exclusively experimental data). However, it may be possible to leverage transfer learning techniques to incorporate separate datasets spanning multiple levels of the data hierarchy (represented in Fig. 1 using arrows). For example, in a setting where a limited amount of labeled experimental data is available, we can improve synthetically pretrained models by incorporating a fine-tuning step [1]. In this study, we analyze the extent to which transfer learning can enhance the capability to perform radioisotope identification in a target domain where data might be limited.

Obtaining a large, well-characterized, experimental dataset proved to be a prohibitive obstacle for this research. Since the primary goal of this study is to explore different data science techniques, we instead use a Geant4 Monte Carlo simulated dataset as the target domain for this analysis [2]. For the source domain, we generated spectra using GADRAS, which is a fast, deterministic tool for synthetically calculating gamma-ray detector responses [3]. While the results of this analysis do not guarantee that these methods would extend to experimental data, this study serves as a powerful proof of concept to adapt a gamma spectral classifier from one data domain to another using modern transfer learning techniques.

2. Background

As radioactive material decays, gamma rays are emitted with energies specific to particular decay pathways of the present radioisotopes [4]. The measurement of these gammas yields a gamma spectrum, which is a histogram of detected gamma energies over a measurement period. Traditional techniques for gamma spectral analysis search for peaks in a measured gamma energy spectrum, which can subsequently be associated with particular decay energies of certain radioisotopes [5, 6, 7]. These methods typically include numerous time-consuming preprocessing steps and require close monitoring by an expert spectroscopist [8, 9, 10]. Furthermore, classical approaches struggle in the presence of thick shielding or when the spectrum contains many overlapping material signatures.

Machine learning presents a promising alternative for improving the speed and accuracy of material classification using gamma spectroscopy [11, 12, 13, 14, 15, 16, 17]. Due to the challenges associated with obtaining a large experimental dataset, most existing literature heavily leverages synthetic data to train classification models. However, deploying a model trained on synthetic data to a real-world setting can be risky, since the ability for such models to generalize is inherently limited by the sim-to-real gap. While steps can be taken to minimize the domain gap through sophisticated data curation techniques, models trained solely on synthetic data will always experience some performance degradation due to a variety of unpredictable nuances in collecting real-world data.

3. Methodology

3.1. Dataset Curation

In this analysis, we simulated a dataset of gamma spectra using both GADRAS and Geant4. In Geant4, we simulated the gamma emission spectra of 55 individual radioisotopes by dissolving each isotope uniformly within a scintillation cocktail. A high-purity germanium (HPGe) detector was placed one meter from the source, and the energy of all incoming gamma rays was recorded and binned to create a gamma spectrum. The simulations were repeated using a mix of different scintillation cocktails and HPGe detector models in order to capture additional variance which may be present in a realistic environment. We leveraged the G4ARES simulation framework to improve estimations of gamma cascade summing corrections [18]. As post-processing steps, we applied a low-energy cutoff and performed Gaussian energy broadening over each spectrum. Once these template spectra were simulated, we created mixed spectra by arbitrarily summing up to 15 individual spectra together with random proportions. We subsequently added background (cosmic, potassium-40, radium-226, and thorium-232) and Poisson noise to generate a diverse dataset of around one million spectra. Finally, the spectra were ℓ_1 normalized by dividing by the total counts. As a point of clarification, we seldom used the entire dataset for model training, but rather subsets of varying sizes, since the objective of this research is to benchmark model performance as a function of dataset size.

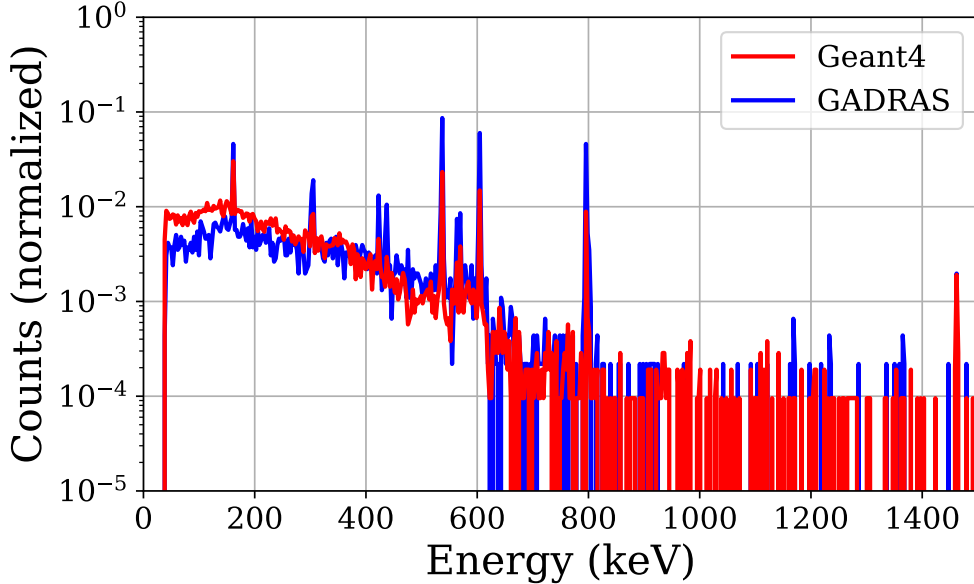


Figure 2: Example training spectrum containing a mixture of barium-140 and cesium-134. Both GADRAS and Geant4 spectra are shown after adding background and Poisson noise. The spectral shapes are similar, but there is a clear shift between the GADRAS and the Geant4 simulations, highlighting the gap between the source and target domains.

We followed a similar sequence of steps for generating GADRAS data, first simulating 55 template spectra using a default 95% efficiency HPGe detector. The spectra were then mixed, background-added, and Poisson resampled, all performed using the PyRIID SeedMixer and StaticSynthesizer classes [19]. A total of ≈ 1.4 million mixed spectra were produced, divided into separate training, validation, and testing sets. The spectra were downsampled to 512 uniform energy bins spanning from 0 keV to 1500 keV in order to speed up runtime and improve memory efficiency. An example gamma spectrum containing a mixture of barium-140 and cesium-134 is shown in Fig. 2 for both the GADRAS and the Geant4 simulations.

Our research objective with these datasets is to determine whether we can apply knowledge learned from one domain to improve performance in a different domain using transfer learning techniques. It is inexpensive to produce large volumes of synthetic data using GADRAS, so we refer to this dataset as the source domain. For a real-world application, the target domain would be experimental spectra that the researcher aims to classify. Since we were unable to acquire an experimental dataset, we instead use the Geant4 dataset as the target domain in this analysis for algorithmic benchmark purposes. As an aside, the source domain for a real-world application does not necessarily have to be GADRAS if an alternative preferred dataset is available (i.e., generated using Monte Carlo simulation tools such as Geant4 or MCNP [20]).

3.2. Model training and testing

The downstream task of this study is to perform multi-label proportion estimation. For a given gamma spectrum, each of the 55 radioisotope classes may or may not be present, and the presence of each isotope is represented as a proportion between 0 and 1. The proportions of all materials in a given spectrum sum to

unity. For this reason, we chose a softmax activation function and a cross-entropy loss function, where we interpret the output of the softmax function as the predicted proportion of the associated radioisotope. Prior literature also considers a sparsemax loss and activation function, which we found yielded nearly identical results [17, 21].

We consider four different machine learning architectures for this analysis: multilayer perceptrons (MLPs), convolutional neural networks (CNNs), transformers, and long short-term memory networks (LSTMs). MLPs and CNNs are commonly used in prior literature on gamma spectroscopy and serve as simple and effective baselines. Transformers and LSTMs are substantially less common in existing literature and are included to provide a comparison using more advanced architectures. Since each gamma spectrum has 512 bins, we originally treated each spectrum as a sequence of length 512 and feature dimension 1, where the feature was simply the number of counts in the associated bin. However, we found that this yielded poor performance using both the transformer and the LSTM. For these two architectures, we “patched” the gamma spectra by reshaping each spectrum to shape $\left(\left\lfloor \frac{512}{p} \right\rfloor, p\right)$, where p is a hyperparameter. This technique is motivated by past research in computer vision [22]. All hyperparameters across the different models were optimized using a basic grid search. Overall, we found that shallower networks (≤ 2 hidden layers) tended to outperform deeper networks (≥ 3 hidden layers) for the task considered in this study. To ensure consistent total training time across the four architectures, the number of epochs was adjusted to account for their varying sizes.

For each architecture, we trained three classes of models using the datasets generated in Section 3.1. The first class was a single model simply trained on the entire source domain (GADRAS) dataset. The second class of models were trained solely on the target-domain (Geant4) data. Within this class, we trained 20 different models, using a random subset of the Geant4 training data with subset sizes ranging in powers of two from 2^1 to 2^{20} . We expect that these models will outperform the first class of models for large target-domain datasets, and underperform the first class of models for small target-domain datasets. The third class of models were pretrained using the source-domain dataset, and subsequently fine-tuned using the target-domain data. We hypothesize that the transfer learning step performed during the training of the third class of models will result in superior model performance compared to both of the previous model classes for all dataset sizes.

During the transfer learning step, we explored different types of fine-tuning. The simplest transfer learning technique is to continue training all weights in the network on the new dataset using a smaller learning rate (reduced by a factor of 10 in this analysis). An alternative approach is to freeze early layers within the network, and only train the output layer(s). The motivation for the latter method is to preserve the high-level features learned during the pretraining step while also avoiding catastrophic forgetting. This approach is especially popular when retraining networks to perform a different downstream task than they were originally trained on (i.e., fine-tuning a model originally used to identify cars to instead identify trucks). In this study, the downstream task of performing radioisotope proportion estimation is identical between

the pretraining step and the fine-tuning step, and thus we found that freezing the hidden layers and only training the output layer yielded inferior performance to simply fine-tuning the entire network.

4. Analysis

Choosing an evaluation metric for multi-label proportion estimation is less intuitive than for traditional classification problems. In this analysis, we define the absolute proportion error (APE) score, computed by rescaling the mean absolute error to yield a value between 0 and 1, with an output of 1 corresponding to perfect ground truth reconstruction. Explicitly,

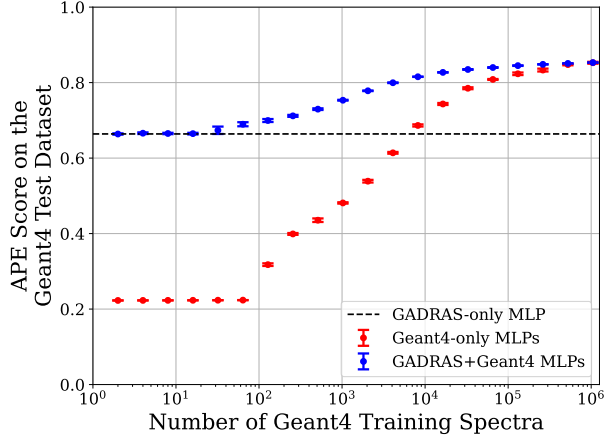
$$\text{APE score} := 1 - \frac{1}{2N} \sum_{i=1}^N \sum_{j=1}^M |y_{\text{pred},i,j} - y_{\text{true},i,j}| \tag{1}$$

$$\sum_{j=1}^M y_{\text{pred},i,j} = 1, \quad \sum_{j=1}^M y_{\text{true},i,j} = 1.$$

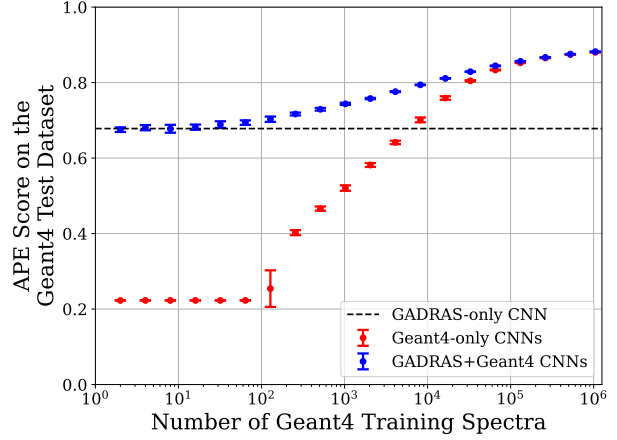
In Eq. 1, N is the number of spectra in the testing dataset, $M = 55$ is the number of radioisotope classes, and y_{pred} and y_{true} are $N \times M$ matrices of the predicted and true proportion labels, respectively. In Fig. 3, we calculate the APE score for each of the three classes of models as a function of the size of the Geant4 training dataset. We show the results using an MLP architecture in Fig. 3a, using a CNN architecture in Fig. 3b, using a transformer architecture in Fig. 3c, and using an LSTM architecture in Fig. 3d. Uncertainties are computed by retraining each model six times with different random weight initializations and randomly drawn Geant4 training samples, and subsequently computing the sample standard deviation of the resulting APE scores.

In all cases, the models that were only trained on Geant4 data (red error bars) perform poorly in the limited data regime ($\lesssim 10^4$ spectra). In the high data regime ($\gtrsim 10^5$ spectra), the models trained on Geant4 data outperform the GADRAS-only model (dashed line), highlighting the clear gap between the source domain and the target domain. Across all architectures, the models that were pretrained on GADRAS and fine-tuned using Geant4 (blue error bars) yield the best APE scores. As we would expect, the performance of the fine-tuned models approaches that of the GADRAS-only model for low amounts of Geant4 data, and similarly approaches that of the Geant4-only models for high amounts of Geant4 data. Importantly, in the intermediate domain ($\approx 10^4$ spectra), the fine-tuned models show substantially improved APE scores compared to both the GADRAS-only and Geant4-only models, suggesting transfer learning offers the most practical use when a moderate amount of data is available.

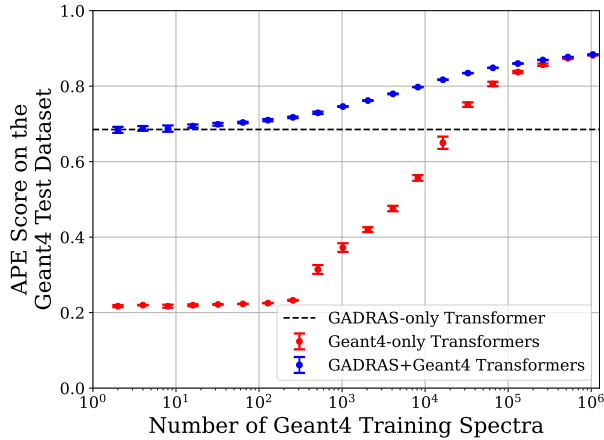
We quantitatively summarize the results of Fig. 3 in Table 1, where we explicitly record the APE scores using an intermediate dataset size of ≈ 8000 Geant4 samples. Across all architectures, we observe that the model pretrained with GADRAS and fine-tuned using the Geant4 samples substantially outperforms models that were trained on only GADRAS data or only Geant4 data. We see minimal variation in computed APE



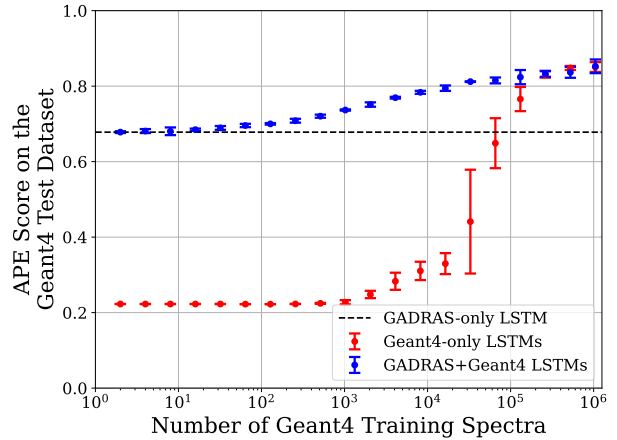
(a) APE score on the Geant4 testing dataset as a function of Geant4 training dataset size using an MLP architecture.



(b) APE score on the Geant4 testing dataset as a function of Geant4 training dataset size using a CNN architecture.



(c) APE score on the Geant4 testing dataset as a function of Geant4 training dataset size using a transformer architecture.



(d) APE score on the Geant4 testing dataset as a function of Geant4 training dataset size using an LSTM architecture.

Figure 3: Calculating the APE score (Eq. 1) on the Geant4 test dataset as a function of the Geant4 training dataset size using different model classes and architectures. The red error bars depict models that were trained from scratch using Geant4 data, the dashed black line depicts a model that was trained using only GADRAS data, and the blue error bars depict models that were pretrained using GADRAS data and then fine-tuned using Geant4 data. Results are shown using four different architectures: MLPs (top left), CNNs (top right), Transformers (bottom left), and LSTMs (bottom right). Uncertainties are estimated by calculating the sample standard deviation across six repeated trials for each dataset size. In all cases, the fine-tuned models yield the best APE scores. We report similar findings using alternative evaluation metrics.

Model Architecture	GADRAS-only model APE score	Geant4-only model APE score	GADRAS+Geant4 model APE score
MLP	0.664	0.686 ± 0.006	0.815 ± 0.001
CNN	0.678	0.701 ± 0.013	0.794 ± 0.001
Transformer	0.685	0.557 ± 0.015	0.797 ± 0.001
LSTM	0.678	0.310 ± 0.048	0.784 ± 0.008

Table 1: APE scores (Eq. 1) of the three model classes using different architectures, evaluated on the Geant4 test dataset. Here, we consider an intermediate dataset size of ≈ 8000 Geant4 spectra. In most cases, the models trained using GADRAS show similar performance to the models trained using Geant4, indicating that the increased quantity of GADRAS samples ($\approx 1e6$ versus $\approx 8e3$) compensated for the out-of-distribution testing environment. The exceptions are the Geant4-only transformer and LSTM models, since these architectures require larger quantities of data to train an effective model. In all cases, the models that were pretrained using GADRAS and fine-tuned using the Geant4 spectra yield the best APE scores. Uncertainties represent a 95% confidence interval.

scores across different architectures, with the exception of the transformer and LSTM Geant4-only models, which perform significantly worse due to the reliance of these models on larger datasets.

Another valuable takeaway of this research is that, after pretraining a model, the subsequent fine-tuning step is substantially faster than training a model from scratch on the same target-domain dataset size. This result is highlighted in Fig. 4, where we demonstrate that using an MLP architecture, a GADRAS-pretrained model required an order of magnitude fewer epochs to converge compared to a model trained from scratch using only Geant4 data. This result demonstrates that using pretrained models can substantially reduce the computational burden of training models, particularly if a model needs to be frequently retrained. This finding is especially pertinent if pretrained models become publicly available in the field of gamma spectroscopy, much like they are in other research domains.

5. Conclusion

In this analysis, we discuss a framework for applying transfer learning techniques to improve the classification performance of machine learning models in a target domain where access to data is limited. We pretrain a model using a synthetic dataset simulated with GADRAS, and subsequently fine-tune the model to perform multi-label proportion estimation in a different target domain, simulated in Geant4. Four different architectures (MLP, CNN, Transformer, LSTM) are considered, all demonstrating similar improvement in APE score after fine-tuning. This result demonstrates that fine-tuning a model that had been pretrained using synthetic data can yield improved performance in an application scenario where data is available but scarce. Future research should apply these techniques to experimental datasets to verify their real-world applicability, while also exploring alternative methods for improving generalization, such as domain transfer, retrieval-augmented generation (RAG), or optimal transport.

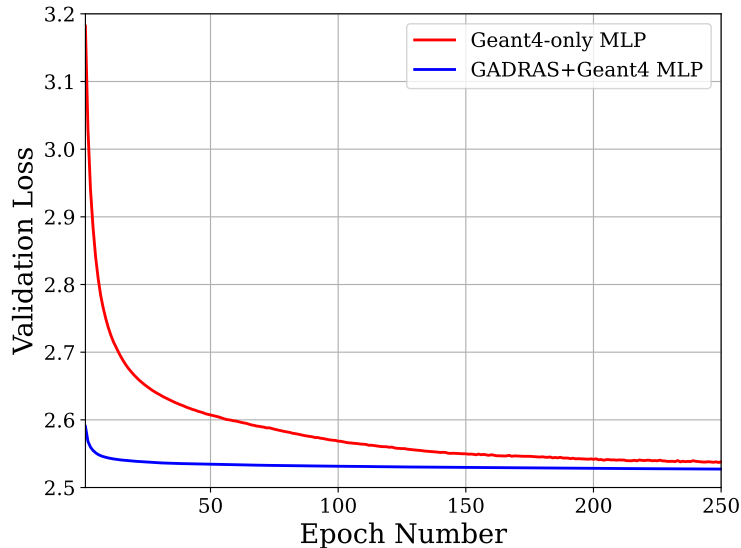


Figure 4: Comparing the validation loss of a trained-from-scratch MLP to a GADRAS-pretrained MLP as a function of epoch number. We observe that the pretrained model converges substantially faster (≈ 20 epochs) compared to the trained-from-scratch model (≈ 200 epochs).

6. Acknowledgements

This research was supported by the Laboratory Directed Research and Development Program at Pacific Northwest National Laboratory, a multiprogram national laboratory operated by Battelle for the U.S. Department of Energy under contract DE-AC05-76RLO1830. Peter Lalor is grateful for the support of the Linus Pauling Distinguished Postdoctoral Fellowship. The authors would like to acknowledge Alex Hagen and Tyler Morrow for their useful suggestions and feedback. The authors declare no conflict of interest.

References

- [1] E. T. Moore, J. L. Turk, W. P. Ford, N. J. Hoteling, L. S. McLean, Transfer learning in automated gamma spectral identification (2020). [arXiv:2003.10524](https://arxiv.org/abs/2003.10524).
URL <https://arxiv.org/abs/2003.10524>
- [2] J. Allison, K. Amako, J. Apostolakis, P. Arce, M. Asai, T. Aso, E. Bagli, A. Bagulya, S. Banerjee, G. Barrand, et al., Recent developments in geant4, Nuclear Instruments and Methods in Physics Research Section A: Accelerators, Spectrometers, Detectors and Associated Equipment 835 (2016) 186–225. [doi:10.1016/j.nima.2016.06.125](https://doi.org/10.1016/j.nima.2016.06.125).
URL <https://www.sciencedirect.com/science/article/pii/S0168900216306957>
- [3] D. J. Mitchell, L. Harding, G. G. Thoreson, S. M. Horne, Gadras detector response function., Tech. rep., Sandia National Lab.(SNL-NM), Albuquerque, NM (United States) (2014).
- [4] G. F. Knoll, Radiation detection and measurement, John Wiley & Sons, 2010.
- [5] T. E. Sampson, Plutonium isotopic analysis using pc / fram (2007).
URL <https://api.semanticscholar.org/CorpusID:34732969>
- [6] Canberra Industries, Inc., Genie™2000 Spectroscopy Software, Canberra Industries, Inc., Meriden, CT, USA, operations, Version 3.1, Document No. 9233652F (2006).
URL <http://www.canberra.com>
- [7] Los Alamos National Laboratory, PeakEasy Software, Los Alamos National Laboratory, version 5.21. (2023).
URL <https://peakeasy.lanl.gov>
- [8] E. Leonard, USDOE, Peak map, version 1.2 (10 2020). [doi:10.11578/dc.20201102.3](https://doi.org/10.11578/dc.20201102.3).
URL <https://www.osti.gov/biblio/1696965>
- [9] M. Darweesh, S. Shawky, Study on the performance of different uranium isotopic codes used in nuclear safeguards activities, Heliyon 5 (4) (2019) e01470. [doi:10.1016/j.heliyon.2019.e01470](https://doi.org/10.1016/j.heliyon.2019.e01470).
URL <https://www.sciencedirect.com/science/article/pii/S2405844018368932>
- [10] M. Croce, D. Becker, K. Koehler, J. Ullom, Improved nondestructive isotopic analysis with practical microcalorimeter gamma spectrometers (04 2021). [doi:10.48550/arXiv.2104.03376](https://doi.org/10.48550/arXiv.2104.03376).
- [11] D. Liang, P. Gong, X. Tang, P. Wang, L. Gao, Z. Wang, R. Zhang, Rapid nuclide identification algorithm based on convolutional neural network, Annals of Nuclear Energy 133 (2019) 483–490. [doi:10.1016/j.anucene.2019.05.051](https://doi.org/10.1016/j.anucene.2019.05.051).
URL <https://www.sciencedirect.com/science/article/pii/S0306454919303044>
- [12] A. Khatiwada, M. Klasky, M. Lombardi, J. Matheny, A. Mohan, Machine learning technique for isotopic determination of radioisotopes using hpge gamma-ray spectra, Nuclear Instruments and Methods in Physics Research Section A: Accelerators, Spectrometers, Detectors and Associated Equipment 1054 (2023) 168409. [doi:10.1016/j.nima.2023.168409](https://doi.org/10.1016/j.nima.2023.168409).
URL <https://www.sciencedirect.com/science/article/pii/S0168900223003996>

- [13] M. Kamuda, J. Zhao, K. Huff, A comparison of machine learning methods for automated gamma-ray spectroscopy, *Nuclear Instruments and Methods in Physics Research Section A: Accelerators, Spectrometers, Detectors and Associated Equipment* 954 (2020) 161385, symposium on Radiation Measurements and Applications XVII. doi:10.1016/j.nima.2018.10.063.
URL <https://www.sciencedirect.com/science/article/pii/S0168900218313779>
- [14] K. J. Bilton, T. H. Y. Joshi, M. S. Bandstra, J. C. Curtis, D. Hellfeld, K. Vetter, Neural network approaches for mobile spectroscopic gamma-ray source detection, *Journal of Nuclear Engineering* 2 (2) (2021) 190–206. doi:10.3390/jne2020018.
URL <https://www.mdpi.com/2673-4362/2/2/18>
- [15] T. Grimes, B. A. Wilson, R. W. Gladen, J. Dermigny, B. B. Cipiti, N. Shoman, Neural assessment of non-destructive assay for material accountancy, *Institute of Nuclear Materials Management (INMM)* (2021).
- [16] A. Van Omen, T. Morrow, A semi-supervised learning method to produce explainable radioisotope proportion estimates for nai-based synthetic and measured gamma spectra (2 2024). doi:10.2172/2335904.
URL <https://www.osti.gov/biblio/2335904>
- [17] A. Van Omen, T. Morrow, C. Scott, E. Leonard, Multilabel proportion prediction and out-of-distribution detection on gamma spectra of short-lived fission products, *Annals of Nuclear Energy* 208 (2024) 110777. doi:10.1016/j.anucene.2024.110777.
URL <https://www.sciencedirect.com/science/article/pii/S0306454924004407>
- [18] B. Archambault, B. Pierson, B. Loer, G4ares-geant4 advanced radio-emission simulation framework, available from <https://gitlab.pnnl.gov/ares/g4ares> [accessed November 20, 2024] (2023).
- [19] T. Morrow, N. Price, T. McGuire, Pyriid v.2.0.0, [Computer Software] (apr 2021). doi:10.11578/dc.20221017.2.
URL <https://doi.org/10.11578/dc.20221017.2>
- [20] F. B. Brown, R. Barrett, T. Booth, J. Bull, L. Cox, R. Forster, T. Goorley, R. Mosteller, S. Post, R. Prael, et al., Mcnp version 5, *Trans. Am. Nucl. Soc* 87 (273) (2002) 02–3935.
- [21] A. Martins, R. Astudillo, From softmax to sparsemax: A sparse model of attention and multi-label classification, in: *International conference on machine learning*, PMLR, 2016, pp. 1614–1623.
- [22] A. Dosovitskiy, L. Beyer, A. Kolesnikov, D. Weissenborn, X. Zhai, T. Unterthiner, M. Dehghani, M. Minderer, G. Heigold, S. Gelly, J. Uszkoreit, N. Houlsby, An image is worth 16x16 words: Transformers for image recognition at scale (2021). arXiv:2010.11929.
URL <https://arxiv.org/abs/2010.11929>